A Role for Dinuclear Aluminum Amidinate Complexes in Ethylene Polymerization?

Robert J. Meier

DSM Research, P.O. Box 18, 6160 MD Geleen, The Netherlands

Eckhard Koglin

Institute of Applied Physical Chemistry (IPC), Research Center Jülich, D-52425 Jülich, Germany

Received: December 31, 2000

Aluminum amidinate species, found to be active in ethylene polymerization, have been studied using a variety of computational methods, including semiempirical (AM1), Hartree−Fock and density functional theory type calculations, and first-principles MD simulations. In agreement with recently reported experimental observations, we find that for all pairs of experimentally studied substituents, dinuclear amidinate structures are very stable toward decomposition. However, with respect to the structure of the active ethylene catalyst, for the most stable dinuclear structures, sterically crowding substituents inhibit insertion through a very high-energy barrier, whereas for noncrowding systems, chain termination by β-hydrogen transfer is likely to dominate over insertion. From finite temperature dynamics simulations, we observe strong fluctuations in the length of the bond bridging the two amidinate rings. It is suggested that the lengthening of that bond relaxes the steric constraints, lowering the barrier for insertion while still forcing the growing alkyl chain to adopt an orientation which inhibits rapid chain termination. Thus, effects explicitly related to finite (nonzero) temperature seem necessary to account for the catalytic activity of these amidinates. Finally, the present study clearly indicates that it is necessary to model the real catalyst, including bulky substituents if present, to arrive at a proper understanding of structure and activity.

Introduction

Most olefin polymerization catalysts have a transition metal or a lanthanide in the active center, which in many cases is cationic in nature. Consequently, the charge on the metal center may be an important factor in relating structure to catalytic activity. Very recently, however, Grubbs et al.[1] have reported polymerization activity for a neutral Ni-based complex. Especially in the field of homogeneous catalysis, such a surprise is not unique, and this partly reflects our still relatively poor understanding of if and why a species shows catalytic behavior. Many metals now seem to be able to do the job, i.e., exhibit catalytic behavior, as long as one finds the right ligand for catalytic activity to come to expression. Moreover, although at first sight this may seem to inhibit catalytic activity for steric reasons, in practice many active catalysts have very bulky ligands.

Another interesting recent finding was the observation by Jordan et al. that relatively simple cationic aluminum complexes, $\{RC(NR')_2\}AlMe^+$, were found to be active catalysts in ethylene polymerization.[2] Polyethylene (PE) with molecular weight (Mw) over 200 000 has been obtained. Jordan and co-workers have been continuing their experimental work on other aluminum-based compounds,[3−6] as well as on corresponding Ga-based complexes.[7] Moreover, Gibson et al. have reported on alkyl aluminum ethylene polymerization catalysts based on monoanionic N,N,N-pyridyliminoamide ligands.[8] It has been known for a very long time that simple aluminum compounds such as AlR_3 can act as a catalyst for the oligomerization of ethylene,[9] but real polymerization using this type of species as a catalyst has been problematic due to rapid chain termination. Despite the fact that ethylene insertion rate can be high, it is the relative ratio of chain propagation (subsequent monomer insertions) and chain termination processes that determine whether oligomers or polymers are formed. Absolute insertion rate determines the quantity of product per unit time, and termination versus propagation rate determines whether oligomer or polymer is formed. More recently, however, it was found that even aluminum alkyl species can, when the polymerization is carried out at room temperature, produce high-molecular-weight polyethylene.[10] Polymerization activity as such is not surprising for aluminum based species, e.g., tetraphenylporphyrin aluminum complexes act as cyclic ether ring-opening catalysts with properties of a living polymerization.[11]

Whereas it has thus been demonstrated from polymerization experiments that certain aluminum amidinate complexes are active ethylene polymerization catalysts, it is not understood[7] what the active species is. Moreover, only a fraction of the Al sites was found to be active.[12] For the Al-amidinates, initially[2] the mononuclear cationic species **I** was considered to be the active catalyst. This seemed supported by the first theoretical study[13] on a model for this catalyst, i.e., $\{RC(NR')_2\}AlMe^+$, with $R = R' = Me$, although the true experimental systems reported by Jordan have at least $R' = {}^iPr$. The calculated barrier of about 25 kcal/mol for ethylene insertion in the mononuclear aluminum complex **I** was found to be in good agreement with the barrier abstracted from experimental polymer yield (22−24 kcal/mol). More recent theoretical work,[14] involving high-level ab initio calculations up to the CCSD level on the mononuclear aluminum amidinate with $R = R' = H$, clearly suggests, however, that the mononuclear species may be inactive as polymerization catalyst, for chain termination by β-hydrogen transfer is energetically more favorable than ethylene insertion.

10.1021/jp004597g CCC: $20.00
Published on Web 03/24/2001

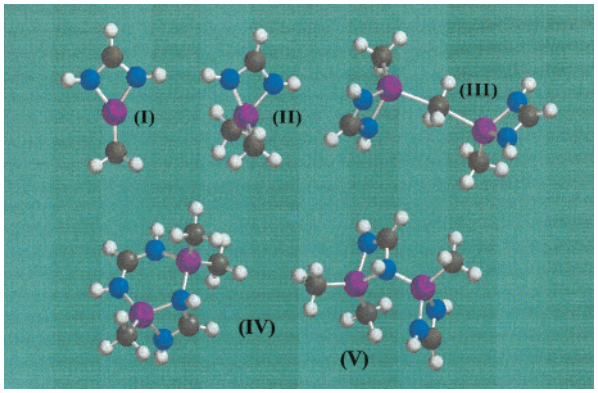

Figure 1. Structures of the mono- and dinuclear aluminium amidinate species studied in this paper. Structure **II** is neutral; all other species have a +1 charge. Color code: aluminium (purple), nitrogen (blue), carbon (black), and hydrogen (white).

In addition, a renewed interpretation of NMR results[7] revealed the predominant presence of dinuclear aluminum amidinate complexes, e.g. complexes **IV** or **V**, formed from the co-addition of cationic species **I** and the neutral species **II**. Then the question arises whether a minor fraction of mononuclear aluminum amidinate or a dinuclear aluminum complex is the active species in polymerization. Finally, from private communications, it became apparent that some investigators think that an impurity of, e.g., a Ti-complex, could be the reason for the observed polymerization activity of the aluminum complexes. Because the activity is low compared to that for a Ti-based active catalyst, only a small amount of an appropriate Ti-based complex could explain the experimental polymerization activity.

From this summary of results on aluminum amidinate systems reported thus far, it is easily concluded that further work is required to understand the structure of the active catalyst and the catalytic activity and, when a structure is proposed, why chain termination does not dominate chain propagation for that species. In the present paper, we will make an attempt to clarify the situation using molecular modeling techniques. We will also discuss the aluminum complexes with "real-life" ligands, i.e., not only simplified ligand systems in order to keep the calculations more feasible. To overcome possible heavy demands on computational power, we will use both first-principles (Car-Parrinello), ab initio (Hartree−Fock and MP2), and density functional theory (DFT-BP86) methods, as well as semiempirical quantum mechanical methods (AM1), and even simple visualization techniques, depending on the issue and the appropriateness of the methods.

Starting Point, Assumptions, and Outline

In view of the considerations mentioned in the Introduction, it is not a priori clear where to start. It may altogether not even be for sure that aluminum amidinate systems are active in olefin polymerization. Therefore, we first want to draw some preliminary conclusions from previously reported work before coming up with a working plan. If it is a Ti-based complex which is the active species, a modeling study of the Al−amidinate systems should reveal these systems are inactive (high termination rate compared to propagation rate, or simply a very high insertion barrier). We do believe that there is a good chance, however, that some of the amidinates are actually catalytically active in polymerization: activity has been reported by various groups[2,7,8,15], but more importantly, amidinates with different alkyl substituents exhibit very distinct polymerization behavior from nonactive to reasonably active polymerization catalysts. Experimentally,[12] it has been observed that whereas $\{MeC(NR)_2\}AlMe^+$-based species are not active in polymerization or only show trace activity, by far the most active species in the series is $\{^tBu(N^iPr)_2\}AlMe^+$, whereas $\{^tBuC(N^tBu)_2\}AlMe^+$ does not show any or very little activity. These observations suggest that it is not likely that an impurity Ti-species is responsible for polymerization activity in only some of the aluminum amidinate samples. Furthermore, even for $AlEt_3$,, which has traditionally been considered as not active in polymerization, recent work[16] has revealed that it can be used to polymerize polyethylene, while it was carefully checked that no transition metal impurities (Ti, Zr, and V) were found present. On the basis of these arguments, we expect an aluminum amidinate related species to be active as an ethylene polymerization catalyst. Because in real experimental catalysis the lifetime of a catalysts, i.e., catalyst degradation, is of eminent importance, it is always possible that some species are not active because they are degraded products. This may seriously complicate the elucidation of trends in activity in a series of, albeit related, species. This problem, however, cannot be overcome in present modeling studies.

In the above, we have mentioned that Talarico et al.[14] have reported a very good quality set of first-principles theoretical results, revealing that the mononuclear aluminum amidinate with $R = R' = H$ is not an active polymerization catalyst because chain termination by β-hydrogen transfer is much faster than ethylene insertion. We adopt that conclusion and will rediscuss it later within the context of the experimental systems which have alkyl ligands rather than $R = R' = H$. This finding, along with the referenced NMR results suggesting the presence of dinuclear aluminum amidinate complexes, requires a study of the stability of dinuclear amidinate species. Our first goal therefore is to study the relative stability of various dinuclear aluminum amidinate species compared to dissociation into mononuclear aluminum amidinates. The model system $\{RC(NR')_2\}AlMe^+$ with $R = R' = Me$ is studied using ab initio and DFT methods, whereas the experimentally studied species with $R' = {}^i$Pr or ^{t}Bu and the system for which $R = R' = {}^t$Bu are subjected to semiempirical calculations using the AM1 method.

After the evaluation of the calculational results obtained, we will reconsider the situation. When suggestions for active species can be made, it will be necessary to discuss the possible importance of the chain termination process through β-hydrogen transfer for that particular species.

Computational Details

Static Hartree−Fock (HF), MP2 ,and density functional theory (DFT) calculations were performed using Gaussian94[17] running on a CRAY T90 and DGauss 4.1[18] implemented on a Cray T3E−1200, respectively, both machines being located at the Forschungszentrum Jülich, Germany. A 6-31G* basis set was employed for all atoms, and in addition, in DGauss the A1 auxiliary basis was used.

All other calculations were performed at DSM Research. For the semiempirical AM1[19] and some of the DFT calculations, we used the SPARTAN Pro program[20] running on an IBM dual-processor Netfinity Pentium III 600 MHz computer system. The first-principles molecular dynamics calculations are based on the original Car−Parrinello (CP) code,[21,22] running on an IBM 3CT workstation. Further computational details include the use of the Perdew−Zunger parametrization of the exchange-correlation functional, along with nonlocal corrections according to Perdew and Becke, known as PB86.[23] Soft Vanderbilt pseudopotentials were employed, except for Al. For references

to original papers, we also refer to one of our earlier papers.[24] A 15 Rydberg cutoff energy has been used; recent experience shows that such a small cutoff is often sufficient.[13,25,26] The time-step was 10 au (0.242 fs), the electronic mass 600 a.u. The Car−Parrinello method was originally devised using a plane-wave basis set and, thus, uses a unit cell and periodic boundary conditions. To simulate isolated molecular systems, we should create sufficient vacuum around the molecular complex in a unit cell in order to minimize interactions with the image in neighboring cells. The size of the cell used in the present study (for CP simulations only) was $30 \times 30 \times 30$ or $35 \times 35 \times 35$ bohr^3, depending on the size of the system (size for specific molecules is given below in Results section); 1 bohr equals 0.529 Å.

To study the insertion of ethylene, we have applied a constraint on the relevant C−C distance (the bond to be formed after insertion has completed). Since the product is well-known, there should be no problem applying this methodology. By varying the value of this constrained distance, we obtained the entire reaction profile. For a good estimate for the barrier to insertion to be obtained, the distance steps around the transition state have to be sufficiently small. This is exactly the procedure we have used in previous work on the aluminum amidinate species[13] (see that work for plots of data also referred to later in the present manuscript).

With respect to the accuracy of energies, it is important to mention that differences on the order of a few kilocalories per mole are at the cutting edge of current computational technologies. Therefore, when energies differ by only a few kilocalories per mole, we will call these close in energy. Moreover, as another result of limited accuracy of energies, the relative order of stability of two species is also not a priori correct when the difference is calculated as a few kilocalories per mole only. This should be kept in mind reading the tables and accompanying discussions in the text.

Results

Stability of Dinuclear Aluminum Amidinate Complexes R = R′ = Me. Because no experimental data are available to validate the relative energies for the dinuclear structures, we first evaluate the performance of the computational methods employed to a system for which experimental data is available, e.g. the dimerization of trimethyl aluminum.

The stability of the Al_2Me_6 dimeric form has been claimed in the vapor phase with an enthalpy of dimerization near 20 kcal/mol in favor of the dimeric form,[27,28] but in solution, the degree of dimerization is highly dependent on solvent, temperature, and concentration (see references in Tarazona et al.[29]). Corresponding quantum calculations have been reported by Willis and Jensen[30] and Berthomieu et al.[31] We have performed HF and DFT calculations on the HF-optimized geometry. By comparing to the results reported in ref 31, which involve geometry optimization at the same level as used for final energy evaluation, we conclude, viz. Table 1, that geometry optimization at the HF level is appropriate. In addition, the HF/6-31G* geometry is in appropriate agreement with available X-ray[32,33] and electron-diffraction results,[34] whereas it has also been shown that this level of calculations yields excellent simulated far-infrared spectra when compared to those of the experiment.[29] The relatively bad performance of some of the methods, some HF results (basis set dependence), and the semiempirical AM1 method with respect to evaluation of the dissociation energy is attributed to the way these methods are capable describing the methyl bridge in species such as the trimethyl aluminum dimer and structure **III**. This is further supported by the observation that these methods do not severely underestimate the bonding in the dinuclear species with only normal covalent bonds, viz. structures **IV** and **V**, as we will see below (Table 2). We note, generally speaking, that HF lacks a description of correlation energy, whereas DFT methods do not describe dispersion forces correctly. For the present systems, because both BP86 and MP2 give acceptable absolute values, even for these methyl bridged species, we conclude that these methods (always on a Hartree−Fock optimized geometry) may be used in a comparative study of the dinuclear structures **III**−**V** with varying R,R′. We emphasize that in the present study we are looking for qualitative understanding of catalytic activity, and therefore, at this stage we do not look for very accurate energies. Moreover, we will compare mutually comparable systems, i.e., aluminum amidinates, and partial cancellation of errors may be expected.

TABLE 1: Dissociation Energies, in kcal/mol, for Trimethyl Aluminum According to the Semiempirical AM1 Method, the ab Initio HF and MP2 Methods, and the BP86 DFT Method[a]

method	AM1	HF	BP86	MP2	exp.[35,36]
ref 31		+4.5	+15.5	+20.0	+20.2/+20.4
present work	+4.7	+4.5	+15.2	+21.2	

[a] The 6-31G(d,p) basis set was employed in the work reported in ref 31, the 6-31G(d) basis set in calculations from the present work. Our results involve optimization at the HF level and single-point calculations for the DFT methods.

TABLE 2: Dissociation Energies, in kcal/mol, for Dinuclear Aluminum Amidinate Structures Shown in Figure 1, i.e., R = R′= Me[a]

	method			
structure	AM1	HF/6-31G*	BP86//HF	MP2//HF
(III)	+19	+20	+35	+35
(IV)	+30	+39	+39	+55
(V)	+57	+47	+49	+66

[a] Dissociation is into the mononuclear species **I** and **II**. For the AM1 method, the (μ2-Me)$_2$ bridged structure is not stable but rearranges to an associated configuration consisting of structures **I** and **II**. The (μ2-Me)$_3$ bridged structure is also unstable upon full optimization at the HF level (see text for further eplanation).

The stability of the dinuclear species **III**, **IV** and **V** versus decomposition into **I** + **II** was studied by full geometry optimization at the HF level (cf. Table 2). Because DFT geometry optimizations tend to take a lot longer than the corresponding HF runs, a fact not unknown among practitioners of both type of calculations, we have performed single-point energy calculations using either a DFT method (BP86) or MP2, a post-HF method that accounts for some of the correlation energy. Regarding the methyl bridged species, one can envision three different structure designated as (μ_2-Me), (μ_2-Me)$_2$, and (μ_2-Me)$_3$. The (μ_2-Me) structure corresponds to **III**. The corresponding (μ_2-Me)$_2$ was not found to be stable with respect to formation of the third bridge: an input geometry for the (μ_2-Me)$_2$ structure evolved into the (μ_2-Me)$_3$ structure during geometry optimization. A similar effect was observed for the triply bridged (μ_2-Me)$_3$. Whereas energy minimization initially seemed to lead to a stable structure, forcing it to adopt a geometry which obeys the maximum force and step-size conditions which are default in the Gaussian disrupted the structure, and it evolved into (μ_2-Me), i.e., structure **III**. Thus, the doubly (μ_2-Me)$_2$ and triply (μ_2-Me)$_3$ bridged structures are unstable with respect to transformation into the mono methyl bridged structure **III** and will therefore be disregarded in what follows.

The trend in the numbers obtained by the different theoretical methods for trimethyl aluminum is largely reflected in the results we have obtained for the dinuclear aluminum amidinates. The dissociation energies are higher than those for trimethyl aluminum, but the trend is very much along the same lines. Structures **IV** and **V** do not exhibit the comparatively weaker methyl bridging but more normal covalent type bonds, which is reflected in the observation that the dissociation energy for these structures are very similar for the HF and DFT methods. Both the AM1 and the MP2//HF method yield high dissociation energies, with a trend similar to those of HF and BP86//HF.

In summary, all four methods applied reveal structure **V** as the most stable structure, followed by structure **IV**. Moreover, the relative energies (on the order of 40 kcal/mol compared to dissociated pair) imply that these dinuclear species are very dominantly present in a mixture of structures **I** and **II**. In the next section, we consider the amidinates with more realistic groups R,R′, i.e., systems experimentally studied by Jordan and co-workers.[2,7]

Stability of Dinuclear Aluminum Amidinate Complexes with Bulkier Substituents. In the previous section, the amidinate species considered had R═R′═Me, whereas the species synthesized by Jordan et al., some of which exhibited ethylene polymerization activity, have R′═^{i}Pr or ^{t}Bu and R═Me or ^{t}Bu. Thus, before making any connection between the ab initio calculated stabilities reported in Table 2 and the experimental results from Jordan et al., we should verify whether that the results from Table 2 still stand when the real, experimentally adopted, substituents are considered. Because ab initio geometry optimization is very demanding when performed for all of the substituted species, we have used the semiempirical AM1 method. This allows for energy minimization also for the largest of the structures, and we will test its validity by comparing the order of the relative energies for the simple species $\{RC(NR')_2\}AlMe_2$ with R = R′ = Me for which the ab initio data are available in Table 2 and by comparing some specific changes in the geometry of the amidinate complexes to experimental data reported by Jordan et al.[7]

Table 3 comprises the AM1 calculated heats of formation and relative energies for the experimentally studied amidinate structures R = Me and R′ = ^{i}Pr, the series R = ^{t}Bu and R′ = Pr, and the series R = ^{t}Bu and R′ = ^{t}Bu. Structure **VI** will be discussed later. For the model structure having R = R′ = Me, we find the same trend as those from the ab initio calculated data collected in Table 2, i.e., structures **III**, **IV**, and **V** are all very stable with respect to dissociation, with structure **V** being the most stable form. The mutual energy differences between the structures is more exaggerated in the AM1 data compared to the first-principles data collected in Table 2. Nevertheless, the AM1 data do show substantial stability of the dinuclear structures and the correct relative order and may therefore be used as a qualitative tool to study the aminidates with bulkier substituents. The AM1 calculations reveal the same order of stability for the species having R = Me and R′ = ^{i}Pr. For the next series, however, which has R = ^{t}Bu and R′ = ^{i}Pr, whereas all three structures are still found to be stable with regard to dissociation, now structure **IV** is found to be the most stable dinuclear species. Finally, for the R = R′ = ^{t}Bu structure, **III** is the most stable structure, whereas structures **IV** and **V** feature almost no net association energy as a result of the bulky substituents which cause strong van der Waals repulsion in these crowded structures. Dagorne et al.[7] have reported the following on the basis of X-ray and NMR experiments:

TABLE 3: Dissociation Energies for Dinuclear Aluminum Amidinate Structures Shown in Figure 1, but with Varying Type of Substituents, Based on the Enthalpies of Formation Obtained from Calculations (full geometry optimization) Using the Semiempirical AM1 Method[a]

structure	dissociation energy (kcal/mol)
R = R′ = Me Model System	
I	not appl.
II	not appl.
I + II	not appl.
III	+18.8
IV	+30.2
V	+56.8
VI	+70.9
R = Me and R′ = ^{i}Pr Not Active (trace activity only)	
I	not appl.
II	not appl.
I + II	not appl.
III	+18.6
IV	+34.8
V	+44.8
VI	+57.6
R = ^{t}Bu and R′ = ^{i}Pr Most Active Catalyst	
I	not appl.
II	not appl.
I + II	not appl.
III	+16.9
IV	+29.1
V	+20.8
VI	+30.3
R = R′ = ^{t}Bu Not Active	
I	not appl.
II	not appl.
I + II	not appl.
III	+21.1
IV	+ 4.4
V	− 1.3
VI	+1.2

[a] Dissociation is into the mononuclear species **I** and **II**. Structure **VI**, Figure 2, is an open form of structure **V**.

(i) $\{RC(NR')_2\}AlMe^+$, R = Me and R′ = ^{i}Pr, or R′ = Cy, features dinuclear structure **V**
(ii) $\{RC(NR')_2\}AlMe^+$, R = ^{t}Bu and R′ = ^{i}Pr, features dinuclear structure (**IV**)
(iii) $\{RC(NR')_2\}AlMe^+$, R = ^{t}Bu and R′ = ^{t}Bu, the dinuclear structure, if it exists, is much less stable than that for R′ = ^{i}Pr or Cy.
The results from the AM1 calculations fully support the trend described by Dagorne et al. for the series described under i−iii.

Dagorne et al. have described a rather dynamic behavior of structure **IV** for R = Me and R′ = ^{i}Pr. At temperatures above some −85 ^{o}C, the structure starting from a configuration as shown in Figure 1 evolves through an open structure like shown in Figure 2 into another structure of configuration **IV** but having the other of the two aluminum atoms in the constrained metallacyclobutane ring. AM1 calculations reveal (Table 3) that the open structure **VI** is more stable than its counterpart **V** when R = R′ = Me or R = Me and R′ = ^{i}Pr. However, for R = ^{t}Bu, R′ = ^{i}Pr, and R = R′ = ^{t}Bu, the open structure **VI** is energetically relatively close to the dinuclear structure **IV**. (Close in energy here is used in the sense as that described in the Computational Details section). Qualitatively, this can be appreciated when considering the increasing bulkiness causing destabilization of the sterically crowded structure **V**, whereas a further increase of the bulkiness (R = R′ = ^{t}Bu) causes even structure **IV** to destabilize in favor of structure **III**. Although it needs further study to link the presence of structure **VI** to the NMR data reported by Dagorne et al.,[7] we have found additional

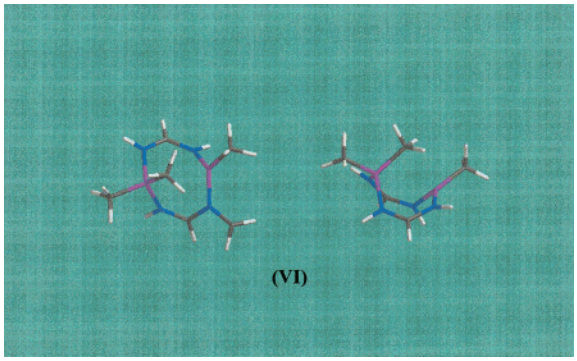

Figure 2. Dinuclear aluminium amidinate structure **VI**, which is a more open version of structure **IV**, displayed in Figure 1. Color code: aluminium (purple), nitrogen (blue), carbon (black), and hydrogen (white).

evidence for the presence of structure **VI**. First, Car−Parrinello-type molecular dynamics simulations, which imply classical treatment of the nuclear motion but full quantum mechanical description of the electronic wave functions, reveal that the open structure **VI** is formed part of the time. Second, even for the neutral equivalent of structure **VI**, with both aluminum centers having two Me groups, the dinuclear ring structure is more stable (25−35 kcal/mol at the HF and the DFT/BP86 level of calculation) compared to the two constituing mononuclear amidinates. Finally, dimerization of neutral indium amidinate $\{HC(NCy)_2\}InMe_2$ in a structure very similar to **VI** for the aluminum amidinate has been reported.[37]

In conclusion, for the sterically less crowded systems, the open structure **VI** seems the most stable structure. This structure is possibly in dynamic equilibrium at finite, but not too low, temperatures with structure **IV**. When crowding increases, structure **V** becomes competitive, whereas for very bulky substituents ($R = R' = {}^tBu$), structure **III** is energetically the most stable form. An important conclusion from this paragraph is that for all pairs of substituents considered there is a dinuclear structure which is considerably more stable compared to dissociation into the mononuclear constituents.

Chain Termination. Before we have a final discussion on the activity of aluminum amidinate species for ethylene polymerization, we first discuss some aspects of chain termination by β-hydrogen transfer. As referred to in the Introduction, despite the fact that an organometallic species can be highly active in insertion and propagation of monomer insertion, when chain termination is more or about as likely, no polymer will be formed. For the amidinate system with $R = R' = H$, Talarico et al.[14] showed that termination by β-hydrogen transfer is more favorable than insertion. However, Jordan's experimental catalysts have at least $R' = {}^i Pr$, i.e., more bulky substituents, and these need therefore be considered also in the process of chain termination.

We suggest the high termination rate for $R = R' = H$ (theoretical result) and the fact that some of the experimental systems do reveal polymerization activity can be understood in the following way. The structure at the top of Figure 3 shows a simple amidinate with ethylene approaching for insertion. This configuration, which is the one at the onset of insertion, has a (Al−)Me hydrogen in proper positioning for β-hydrogen transfer. When the barrier for H-transfer is sufficiently low, this process is dominating and no polymer is formed. However, when a steric barrier is created, as illustrated in the lower part of Figure 3, the growing chain has to be pointing away from the incoming ethylene (which could come from above in this picture) because otherwise (with the alkyl chain pointing upward) the ethylene would be prohibited to approach due to steric hindrance of the amidinate framework. This picture merely serves a more general observation when studying the amidinate series using 3D-molecular models; i.e., crowding at the catalytic center tends to dictate the orientation of the growing alkyl chain, forcing the β-hydrogens to point away from the incoming ethylene. When the system becomes too crowded, however, ethylene insertion itself is prohibited by a high energy barrier, as we will see in the next paragraph.

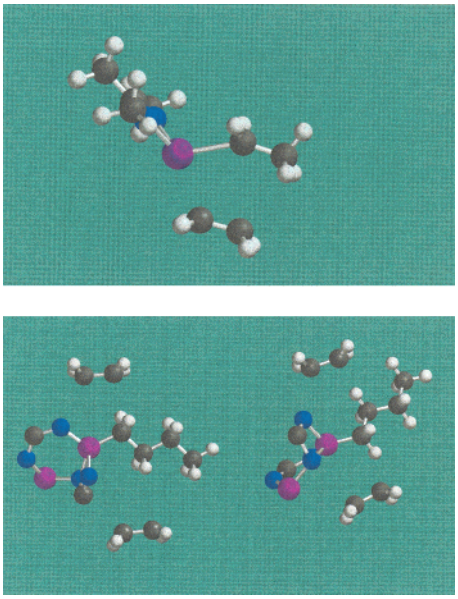

Figure 3. (a, top) Structure illustrating the possibility of β-hydrogen transfer for the mononuclear aluminium amidinate structure. A methyl (β-) hydrogen can easily transfer to the incoming ethylene, provided that the barrier for that process is sufficiently low. According to the calculations by Talarico et al.,[14] the latter is indeed the case, and therefore, no polymerization activity is expected for this species. Color code: aluminium (purple), nitrogen (blue), carbon (black), and hydrogen (white). (b, bottom) Structures illustrating the non-possibility of β-hydrogen transfer to occur in the dinuclear structure **IV**. For clarity, the substituents R,R′ on the amidinate ring have been omitted. The left-hand and right-hand configurations illustrate two different orientations of the growing alkyl chain with respect to the amidinate ring system. *Left-hand structure*: the ethylene coming from "below" can approach a β-hydrogen, but it is sterically hindered to approach the aluminium centre due to the presence of the fused amidinate rings. The ethylene coming from "above" may be able to insert, but it can't possibly approach a β-hydrogen. Thus, β-hydrogen transfer is strongly hindered for steric reasons imposed on the incoming ethylene with respect to the growing alkyl chain. *Right-hand structure*: the same observations as those for the left-hand structure, but the situation is interchanged with respect to the ethylene coming from "above" and that coming from "below". Color code: aluminium (purple), nitrogen (blue), carbon (black), and hydrogen (white).

Ethylene Insertion. In this brief section, we simply quote a few results on ethylene insertion which are relevant to our final discussion on activity of the dinuclear aluminum amidinate species. We emphasize that the aminidate species are essentially the $T = 0$ K structures obtained from very low-temperature dynamics simulations (Car−Parrinello) or full energy minimization using static structure codes (Gaussian, Spartan, and DGauss). The relevance of this aspect will become clear in the subsequent section when we discuss the possible relevance of dynamic structure evolution at finite, elevated, temperature.

In a previous paper,[13] we have studied the insertion of ethylene in a number of amidinate complexes, primarily by applying Car−Parrinello-type simulations (BP86 functional within DFT framework) using low-temperature annealing

techniques to probe minimum-energy structures. For insertion into the model mononuclear amidinate species **I** or insertion of ethylene in the bridging methyl group into structure **III**, including the simple model aluminum amidinate, the barrier for insertion was found to be around 25 kcal/mol. When insertion into the nonbridging Al-Me bond in structure **III** was attempted, the barrier increased by 10 kcal/mol up to a total barrier close to 40 kcal/mol. From new calculations, the barrier for insertion into structure **V** with R = Me and R′ = ^{i}Pr (unit cell size 30 × 30 × 30 bohr^3) was found to involve an estimated barrier of around 50 kcal/mol, which may be understood recognizing both steric crowding and the relative stability of that structure compared to dissociation (Table 3). Thus, whereas for the simple mononuclear amidinate complexes such as structure **I** chain termination is favored over insertion, the barrier for insertion is increasing with increasing crowding of the dinuclear structures.

What we should take from this is that whereas for mononuclear aluminum amidinates termination is more facile than insertion, for the stable dinuclear structure **V** or the bridged species **III**, the barrier is too high to be considered in some form of agreement with reaction rates roughly estimated from experiments (see ref 13 for the quoted numbers). So even when for these dinuclear species termination is less likely than for the mononuclear equivalents, the barrier for insertion is considered too high to make the species account for experimentally observed polymerization behavior.

Discussion: Catalytic Activity of Aluminum Amidinates?

The crucial question we try to address is the catalytic activity of aluminum amidinates. We recall that, according to the experiments reported by Jordan et al., the amidinate {RC(NR′)$_2$}AlMe$^+$ is active in ethylene polymerization for R = ^{t}Bu and R′ = ^{i}Pr but not for the combination R = Me and R′ = ^{i}Pr nor for R = R′= ^{t}Bu. These observations, in combination with the theoretical results presented in the above, suggest a dinuclear aluminum amidinate to be the active catalyst.

We have found that the structures with small substituents, the model system R = R′ = Me, and the experimental system R = Me and R′ = ^{i}Pr, favor structure **V** or **VI**. Structure **V** exhibits a large barrier to insertion (previous section), whereas **VI** is open and is expected to readily facilitate chain termination through β-hydrogen transfer in the same sense as the mononuclear amidinate.[14] The bulkier the structure gets, the more likely the stabilization of structure **IV** becomes, with the possible presence of **VI** at the same time. This bulkiness, however, prevents the insertion of ethylene to be a viable process, from an energetic point of view.

We now face the situation that either a species is not expected active because it is too bulky (high barrier to insertion) or it is not bulky enough to prevent the β-hydrogen transfer termination process to be dominating over insertion. A way out of the dilemma is to consider the nature of the species at realistic conditions, i.e., finite temperature. For a system to overcome a nonnegligible energy barrier, it has to have sufficiently high internal energy. This corresponds to a species in the high-end tail of the Maxwell−Boltzmann velocity distribution. For simulation purposes, one may simulate a species in that segment by imposing increased temperature.[24] We have considered the species structure **IV** with R = Me and R′ = ^{i}Pr (unit cell size 30 × 30 × 30 bohr^3) and structure **V** with R = ^{t}Bu and R′ = ^{i}Pr (unit cell size 35 × 35 × 35 bohr^3). From first-principles Car−Parrinello-type molecular dynamics simulations, we observed the transformation of structure **IV** toward structure **VI**

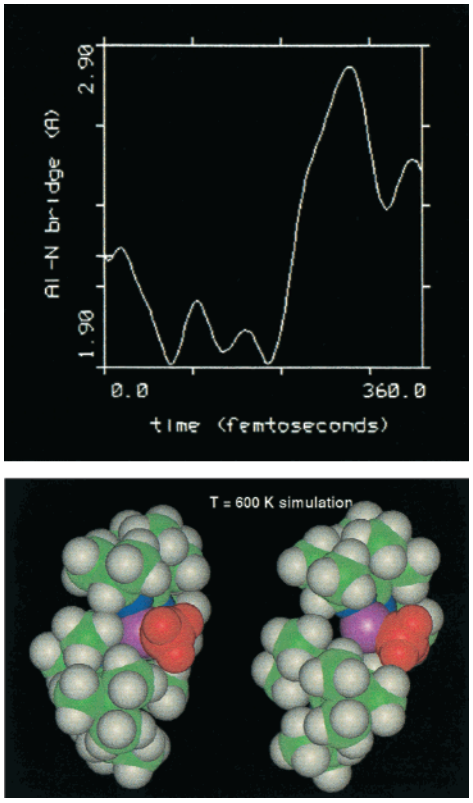

Figure 4. Results from Car−Parrinello-type molecular dynamics simulation on structure **V** dinuclear amidinate, with R = ^{t}Bu and R′ = ^{i}Pr; simulation temperature T = 600 K. Upper plot: time dependence of the bridge Al-N distance. Lower picture: snapshots from the dynamics simulation, showing the structure at t = 0 (left-hand molecular structure) and the geometry at the maximum of the Al−N bridge distance from the upper graph (2.8 Å).

(in that simulation, the temperature was set to T = 600K but was free to vary between 400 and 800 K; except for the beginning of the simulation, actual temperature was in the range of 400−500 K). That latter structure being open is not considered viable for ethylene polymerization for the same reason as that for the mononuclear amidinate with R = R′ = H.[14] Figure 4 shows some of the dynamic features for structure **V**, R = ^{t}Bu and R′ = ^{i}Pr. It is particularly interesting to see that significant lengthening of Al−N bond bridging the amidinate rings is observed, despite the fact of a high dissociation energy. This illustrates that strong fluctuations in bond length are occurring despite strong overall associative forces, and it is the distribution of the internal vibrational energy which determines the relative lengthening of bonds and opening of bond angles. This dynamic behavior of structure **V** opens the possibility for catalytic activity. The Al−N bond lengthening allows for insertion with a lower barrier, such as insertion in the bridging Me in structure **III** (see previous section), whereas the bulky environment still dictates specific orientation of the growing alkyl chain, thereby avoiding rapid chain termination. The most active species from the series of aluminum amidinates studied so far experimentally, {^{t}Bu(NiPr)$_2$}AlMe$^+$, has a comparable energetic stability compared to that of the open dinuclear structure **VI**, which further agrees with Jordan's observation that only part of the aluminum centers is active in the polymerization.[12]

Further support for this interpretation was obtained from calculations applying static DFT energy minimizations (Spartan, BP86 functional) on ethylene insertion in structure **V** and in a structure like **V** but with the Al−N bond connecting the two

TABLE 4: Dissociation Energies for Dinuclear Aluminum Amidinate Structures Having R = Me and R′ = ^{t}Bu, Calculated using the Semiempirical AM1 Method

structure	dissociation energy (kcal/mol)
R = Me and R′ = ^{t}Bu	
Expected Active Catalyst	
I	not appl.
II	not appl.
I + II	not appl.
III	+18.2
IV	+28.7
V	+30.6
VI	+22.2

amidinate rings (see also Figure 4) constrained at 3 Å. This means that whereas for the former, one distance constraint was applied (related to the incoming ethylene), for the latter, an additional, second constraint on the named Al−N bond length was applied. The barrier for the first situation was found to be 41.4 kcal/mol, whereas for the latter, it was found as 33.8 kcal/mol. Thus, we do indeed find a significant reduction in the barrier height for the dynamic structures (Figure 4) exhibiting an increased Al−N distance. Since in the static energy minimization the amidinate rings were able to rotate toward each other while maintaining the Al−N constraint, steric hindrance was higher than in the dynamic structures suggested by Figure 4. Therefore, the lowering of the barrier height by 7−8 kcal/mol is an underestimate.

It may be interesting to note that very recently Keaton et al.[38] have found dinuclear amidinate structures based on Zr, bridged by one or two methyl groups, and have speculated on the effect on polymerization activity of such systems.

Adopting these arguments allows us to make a prediction. From the present investigation, we conclude that a catalytically active amidinate system has a structure which allows for the ethylene to approach the catalytic center without an enormous steric energy term, while at the same time, the substituents force the growing alkyl chain to adopt an orientation which prevents its β-hydrogens to become in close contact to the incoming monomer. Apart from the experimentally studied aluminum amidinate species with R = ^{t}Bu and R′ = ^{i}Pr, we predict that catalytic behavior is to be expected for R = Me and R′ = ^{t}Bu. Using the AM1 method, we obtained the data collected in Table 4. Structure **IV** is close in stability compared to structure **V** (only a few kcal/mol, see comment in Computational Details section), whereas structure **VI** is disfavored. As a consequence, the dynamic structures arising from **V** are expected to exhibit catalytic activity for this species.

Conclusions

Although we realize we have not yet arrived at a full quantitative account for the activity of aluminum amidinates toward ethylene polymerization, we think we have qualitatively captured a picture which agrees with all experimental findings so far and which provides an atomistic account of the factors involved in the catalytic activity of the aluminum amidinate species. Several issues now seem beyond reasonable doubt. According to the various methods of computation we have employed, the dinuclear structures are always much more stable than the corresponding mononuclear aluminum amidinate. For the dinuclear structures, however, very bulky structures inhibit insertion of ethylene, whereas the less bulky structures are relatively open and therefore allow for β-hydrogen transfer to dominate. As a consequence, and this needs further research to fully confirm, finite temperature allows for a lengthening of the bridging Al−N bond in dinuclear structure **V**, allowing for insertion while still enforcing the growing alkyl chain in a direction which does not allow for β-hydrogen transfer.

In conclusion, the overall picture sketched gives a very satisfactory explanation for the polymerization activity of Jordan's aluminum amidinates. Our observations lead to a picture of the catalysis of the aluminum amidinate species which altogether might not be totally surprising: catalysis is a subtle art, often involving a delicate balance. This is precisely what our conclusions suggest: for the species to act as an active polymerization catalyst, the substituents should have a certain crowding in order to avoid chain termination by β-hydrogen transfer to become competitive or even dominating compared to insertion, whereas very crowded structures either do not form the necessary dinuclear structure or, also for steric reasons, inhibit ethylene insertion. Elevated temperature effects are necessary to form the active species.

For the future, we plan further ab initio investigations on the dinuclear species, aiming at further investigation of the model proposed in the present paper. Hopefully. more experimental data will become available for comparison and validation.

Acknowledgment. Prof. Richard Jordan (University of Chicago) is gratefully acknowledged for stimulating discussions and for communicating experimental observations. Dr. Mirko Kranenburg (DSM Research), Meike Reinhold, and Dr. John McGrady and Prof. Robin Perutz (all University of York, U.K.) are gratefully acknowledged for various discussions and shared interest in aluminum amidinate chemistry.

References and Notes

(1) Youngkin, T. R.; Connor, E. F.; Henderson, J. I.; Friedrich, S. K.; Grubbs, R. H.; Bansleben, D. A. *Science* **2000**, *287*, 460.

(2) Coles, M. P.; Jordan, R. F. *J. Am. Chem. Soc.* **1997**, *119*, 8125−8126.

(3) Ihara, E.; Young, V. G.; Jordan, R. F. *J. Am. Chem. Soc.* **1998**, *120*, 8277.

(4) Coles, M. P.; Swenson, D. C.; Jordan, R. F. *Organometallics* **1998**, *17*, 4042.

(5) Radzewich, C. E.; Coles, M. P.; Jordan, R. F. *J. Am. Chem. Soc.* **1998**, *120*, 9384.

(6) Radzewich, C. E.; Guzei, I. A.; Jordan, R. F. *J. Am. Chem. Soc.* **1999**, *121*, 8673.

(7) Dagorne, S.; Guzei, I. A.; Coles, M. P.; Jordan, R. F. *J. Am. Chem. Soc.* **2000**, *122*, 274.

(8) Bruce, M.; Gibson, V. C.; Redshaw, C.; Solan, G. A.; White, A. J. P.; Williams, D. J. *Chem. Commun.* **1998**, 2523.

(9) Lindsay, K. L. Alpha-Olefins. In *Encyclopedia of Chemical Processing and Design*; McKetta, J. J., Cunningham, W. A., Eds. Marcel Dekker: New York, 1977; pp 482−498.

(10) Martin, H.; Bretinger, H. *Makromol. Chem.* **1992**, *193*, 1283.

(11) Aida, T.; Inoue, S. *Macromolecules* **1981**, *14*, 1162.

(12) Jordan, R. F. Private communication. See also refs 2 and 7.

(13) Reinhold, M.; McGrady, J. E.; Meier, R. J. *J. Chem. Soc., Dalton Trans.* **1999**, 487−488.

(14) Talarico, G.; Budzelaar, P. H. M.; Gal, A. W. *J. Comput. Chem.* **2000**, *21*, 398−410.

(15) Experimental results produced at DSM Research.

(16) Kim, J. S.; Wojcinski, L. M., II; Liu, S.; Sworen, J. C.; Sen, A. *J. Am. Chem. Soc.* **2000**, *122*, 5668−5669.

(17) Frisch, M. J.; Trucks, G. W.; Schlegel, H. B.; Gill, P. M. W.; Johnson, B. G.; Robb, M. A.; Cheeseman, J. R.; Keith, T.; Petersson, G. A.; Montgomery, J. A.; Raghavachari, K.; Al-Laham, M. A.; Zakrzewski, V. G.; Ortiz, J. V.; Foresman, J. B.; Cioslowski, J.; Stefanov, B. B.; Nanayakkara, A.; Challacombe, M.; Peng, C. Y.; Ayala, P. Y.; Chen, W.; Wong, M. W.; Andres, J. L.; Replogle, E. S., Gomperts, R.; Martin, R. L.; Fox, D. J.; Binkley, J. S.; Defrees, D. J.; Baker, J.; Stewart, J. J. P.; Head-Gordon, M.; Gonzalez, C.; Pople, J. A. *Gaussian 94*; Gaussian, Inc.: Pittsburgh, PA, 1994.

(18) *Unichem v4.1*; Oxford Molecular: Oxford, 1990.

(19) Dewar, M. S.; Zoebisch, E. G.; Healy, E. F.; Stewart, J. J. P. *J. Am. Chem. Soc.* **1985**, *107*, 3902.

(20) *PC SPARTAN*; Wave function Inc.: Irvine, CA, 2000 (pcsales@wavefun.com; http://www.wavefun.com).
(21) Car, R.; Parrinello, M. *Phys. Rev. Lett.* **1985**, *55*, 2471.
(22) The CP code employed in this work is under development by Dr. Franco Buda and co-workers at the University of Amsterdam, The Netherlands.
(23) (a) Becke, A. D. *Phys. Rev. B* **1988**, *38*, 3098−3100. (b) Perdew, J. P. *Phys. Rev. B* **1986**, *33*, 8822−8824.
(24) Aagaard, O. M.; Meier, R. J.; Buda, F. *J. Am. Chem. Soc*. **1998**, *120*, 7174−7182.
(25) Meier, R. J. *J. Mol. Struct*. (*THEOCHEM)* **1999**, *467*, 79.
(26) Furthmüller, J.; Käckell, P.; Bechstedt, F.; Kresse, G. *Phys. Rev*. **2000**, *B61*, 4576.
(27) Crompton, T. R. *Analysis of Organoaluminium and Organozinc Compounds*; Pergamom Press: Oxford, 1968.
(28) Mole, T.; Jeffery, E. A. *Organoaluminium Compounds*; Elsevier: Amsterdam, 1972; p 94 v.v., and references therein.
(29) Tarazona, A.; Koglin, E.; Buda, F.; Coussens, B. B.; Renkema, J.; van Heel, J.; Meier, R. J. *J. Phys. Chem. B* **1997**, *101*, 4370−4378.
(30) Willes, B. G.; Jensen, K. F. *J. Phys. Chem. A* **1998**, *102*, 2613−2623.
(31) Berthomieu, D.; Bacquet, Y.; Pedocchi, L.; Goursot, A. *J. Phys. Chem. A* **1998**, *102*, 7821−7827.
(32) Lewis, P. H.; Rundle, R. E. *J. Chem. Phys*. **1953**, *21*, 986.
(33) Vranka, R. G.; Amma, E. L. *J. Am. Chem. Soc*. **1967**, *21*, 3121.
(34) Vilkov, L. V.; Mastryukov, V. S.; Sadova, N. I. *Determination of the Geometrical Structure of Free Molecules*; Mir Publishers: Moscow, 1983.
(35) Laubengayer, A. W.; Gilliam, W. F. *J. Am. Chem. Soc*. **1941**, *63*, 477−479.
(36) Henrickson, C. H.; Eyman, D. P. *Inorg. Chem*. **1967**, *6*, 1461.
(37) Zhou, Y.; Richeson, D. S. *Inorg. Chem*. **1996**, *35*, 1423.
(38) Keaton, R. J.; Jayaratne, K. C.; Fettinger, J. C.; Sita, L. R. *J. Am. Chem. Soc*. **2000**, *122*, 12909−12910.